Capillarity

Vol. 16, No. 3, p. 87-94, 2025

Original article

Influence of roughness on spontaneous air-water imbibition in fractures: Insights from mathematical model analysis

Hui Cheng[1,2], Ronghui Lai[3], Jiahao Liu[4], Xurong Zhao[5], Youjin Yuan[3], Fugang Wang[1,2]*

[1]*Key Laboratory of Groundwater Resources and Environment, Ministry of Education, Jilin University, Changchun 130012, P. R. China*
[2]*Jilin Provincial Key Laboratory of Water Resources and Environment, Jilin University, Changchun 130012, P. R. China*
[3]*Hainan Branch, CNOOC China Limited, Haikou 570100, P. R. China*
[4]*Fuxian Oil Production Plant, Shaanxi Yanchang Oilfield Co.Ltd, Yan'an 716000, P. R. China*
[5]*Oil & Gas Technology Research Institute, PetroChina Changqing Oilfield Company, Xi'an 710018, P. R. China*

Keywords:
Spontaneous imbibition
fracture
roughness
fractals
mathematical model

Cited as:
Cheng, H., Lai, R., Liu, J., Zhao, X., Yuan, Y., Wang, F. Influence of roughness on spontaneous air-water imbibition in fractures: Insights from mathematical model analysis. Capillarity, 2025, 16(3): 87-94.
https://doi.org/10.46690/capi.2025.09.03

Abstract:
With the aim to explore the effects of fracture surface roughness on spontaneous imbibition behavior, this study investigates spontaneous air-water imbibition in rough fractures. For this purpose, a mathematical model that comprehensively accounts for fracture surface roughness and gravitational influence is developed. Using the Lambert function, a fully analytical solution for the imbibition height during the spontaneous air-water imbibition process is derived. The results indicate that neglecting fracture surface roughness leads to the overestimation of imbibition rate in model predictions. Moreover, the equilibrium imbibition height is significantly greater than the actual values, which aligns with the experimental observations. As the fractal dimension increases, the rate of imbibition height change decreases, and the imbibition height attained within the same time period is correspondingly reduced. A decrease in contact angle and an increase in interfacial tension both amplify the effect of roughness on imbibition behavior. Additionally, both the equilibrium height and the time required to reach equilibrium decrease with increasing fractal dimension. This research not only deepens the understanding of fluid flow mechanisms in complex fracture networks but also provides essential theoretical support and scientific guidance for engineering applications such as oil and gas extraction.

1. Introduction

Spontaneous imbibition in fractures refers to the phenomenon where a wetting-phase fluid is spontaneously drawn into fractures under capillary forces. This process is not only ubiquitous in nature but also closely related to various engineering applications (Standnes, 2004; Zhang et al., 2023b). For instance, in shale oil and gas development, hydraulic fracturing generates numerous artificial fractures that, along with natural fractures, form complex fracture networks (Yaghoubi, 2019; Khan et al., 2023; Wu et al., 2023). In such cases, the infiltration and distribution of fluids (e.g., fracturing fluid, oil, gas, or groundwater) within fractures have direct implications for resource recovery efficiency, environmental protection, and geological stability (Rezaei and Mousavi, 2019; Zhang and Liu, 2024; Zhang et al., 2024a). Moreover, in fields such as nuclear waste storage and pollutant transport, understanding spontaneous imbibition behavior in fractures is crucial for risk assessment and the development of protective measures

Yandy Scientific Press

*Corresponding author.
E-mail address: chenghui22@mails.jlu.edu.cn (H. Cheng); lairh2@cnooc.com.cn (R. Lai); m15619033029@163.com (J. Liu); zhaoxr21_cq@petrochina.com.cn (X. Zhao); yuanyj22@cnooc.com.cn (Y. Yuan); wangfugang@jlu.edu.cn (F. Wang).

Received July 3, 2025; revised July 29, 2025; accepted August 17, 2025; available online August 22, 2025.

(Zhang et al., 2023a; Hu et al., 2024; Yoon et al., 2024). Therefore, an in-depth investigation into the mechanisms of spontaneous imbibition in fractures is of great significance for optimizing engineering practices, improving resource utilization efficiency and safeguarding the ecological environment.

Various mathematical models have been proposed to describe the phenomenon of spontaneous imbibition (Fries and Dreyer, 2008; Cai et al., 2012; Guo et al., 2024). Some studies focused on the influence of gravity on fluid distribution (Meng et al., 2016; Salam and Wang, 2022; Andersen, 2023), while others emphasized the regulatory effects of fluid and media properties on flow behavior (Shi et al., 2018; Janetti and Janssen, 2022). However, these studies often have limitations. For example, the Lucas-Washburn equation, a classical model for spontaneous imbibition in capillaries, neglects the influence of gravity on the imbibition process (Washburn, 1921; Abd et al., 2019; Wang et al., 2021). Fries and Dreyer (2008) introduced the Lambert function to derive an analytical solution for spontaneous imbibition of the wetting-phase fluid in a gas-saturated single capillary while accounting for gravity. However, these models primarily describe imbibition within matrix pores, whereas the imbibition behavior of wetting-phase fluids in fractures differs significantly from that in the matrix (Wang and Cheng, 2020; Cai et al., 2022). Therefore, it is important to develop theoretical models specifically tailored for spontaneous imbibition.

In recent years, Wang and Cheng (2020) applied the Lambert function to derive an analytical solution for the spontaneous imbibition of wetting-phase fluids in a gas-saturated single fracture while considering the influence of gravity. They further extended their model to obtain an analytical solution for the imbibition height in a two-phase (oil-water) system under the influence of gravity (Cheng and Wang, 2024). However, these models fail to account for the effect of surface roughness on the imbibition process. Furthermore, Brabazon et al. (2019b) proposed an analytical solution for imbibition height that incorporates the impact of roughness, but it did not consider additional influential factors such as gravity and inclination angle.

Fracture surfaces commonly exhibit a certain degree of roughness, which significantly influences fluid flow behavior within fractures (Wolansky and Marmur, 1999; Zhang and Liu, 2024). Natural fractures, formed through geological processes such as plate tectonics and weathering, often feature irregular and highly rough surfaces (Srivastava et al., 2025). Similarly, artificial fractures generated during hydraulic fracturing may develop localized roughness due to interactions between the fracturing fluid and the rock formation (Minakov et al., 2024; Munoz et al., 2025). This surface roughness not only alters fluid flow pathways but also introduces additional flow resistance, thereby affecting the efficiency of spontaneous imbibition (Zhang et al., 2024b; Ma et al., 2025; Torkan et al., 2025). Moreover, the regulatory effects of roughness on fluid flow vary considerably across different scales and morphological characteristics, further increasing the complexity of the problem (Xia et al., 2021; Cai et al., 2025; Zhou et al., 2025). Therefore, incorporating the influence of surface roughness into modeling spontaneous imbibition in fractures is essential for improving model accuracy.

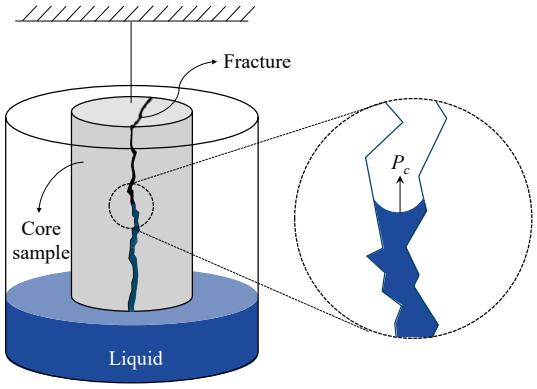

Fig. 1. Schematic diagram of spontaneous liquid imbibition into air-saturated rough fracture.

To sum up, existing imbibition models for fractures either neglect the impact of gravity or fail to comprehensively account for the role of surface roughness in the spontaneous imbibition process. This research gap limits our understanding of fluid imbibition behavior in complex fracture networks. To address this gap, a mathematical model for spontaneous imbibition is derived in this study, which incorporates both roughness and gravity effects. Next, the model is validated against experimental data, and finally, the influence of roughness on spontaneous air-water imbibition in fractures is analyzed. The results provide theoretical support for understanding fluid flow behavior in complex fracture networks while offering scientific guidance for engineering applications such as oil and gas extraction.

2. Mathematical model

In order to simplify the analysis and focus on the influence of fracture roughness on the imbibition process, the following assumptions are made:

1) The flow is assumed to be in the upward direction under the action of capillarity and gravity (Fig. 1).
2) The fracture is initially filled with air, and the effects of air viscosity and density are negligible compared to those of the imbibing liquid.
3) No fluid exchange occurs between the fracture and the surrounding matrix during the imbibition process.
4) Chemical reactions between the fluid and the rock surface are ignored.

Based on the cubic law, the imbibition velocity of liquid spontaneously entering a single fracture under capillary forces can be expressed as (Nazridoust et al., 2006):

$$v = \frac{a^2}{12\mu L_f}\left(\frac{2\sigma\cos\theta_R}{a} - \rho g L_s\right) \tag{1}$$

where v represents the imbibition velocity, a represents the fracture aperture, σ represents the interfacial tension, θ_R represents the actual contact angle between gas-liquid-solid phases during the imbibition process, ρ represents the fluid density, μ represents the fluid viscosity, g represents the acceleration of gravity, L_s represents the straight height of the imbibition front and L_f is the tortuous height of the imbibition front. The

velocity v can be expressed as $\mathrm{d}L_f/\mathrm{d}t$, and the relationship between the straight and tortuous heights of the imbibition front can be expressed as $L_f = \tau L_s$. Then, the above equation can be rearranged as:

$$L_s dL_s = \left(\frac{a\sigma\cos\theta_R}{6\mu x^2} - \frac{a^2\rho g L_s}{12\mu x^2}\right)\mathrm{d}t \tag{2}$$

The above is the basic flow equation for spontaneous imbibition of liquid into a single fracture. Natural fractures typically exhibit rough surfaces. In this study, the rough fracture surface is modeled as being covered by an infinite number of squares, with the relationship between the number of squares and the total fracture surface area following the fractal equation (Family and Vicsek, 1991):

$$N = \left(\frac{\mathcal{L}}{\ell}\right)^{D_f} \tag{3}$$

where N represents the number of squares covering the rough surface, $\mathcal{L}$ represents the side length of the largest square covering the rough surface, ℓ is the side length of the smallest square, and D_f is the fractal dimension of rough surfaces. This assumption has been validated in previous studies as an effective method for characterizing rough fracture surfaces. The rough surface area is denoted as A_R, and the smooth surface area is denoted as A_S.

When the rough fracture surface is covered by N squares with a side length of ℓ, the total surface area of the rough fracture, denoted as A_R, can be expressed as:

$$A_R = N\ell^2 = \ell^{2-D_f}\mathcal{L} \tag{4}$$

In contrast, when the fracture surface is assumed to be a single square with a side length of $\mathcal{L}$ (i.e., a smooth surface), the corresponding fracture surface area, A_S, is given by:

$$A_S = \mathcal{L}^2 \tag{5}$$

Prior research has established that the primary mechanism through which roughness affects the imbibition process is by altering the contact angle (Brabazon et al., 2019b). According to the well-known Wenzel equation (Wenzel, 1936), the actual dynamic contact angle θ_R during fluid flow is related to the static equilibrium contact angle θ_S as follows:

$$\cos\theta_R = r\cos\theta_S \tag{6}$$

where r can be expressed as $r = A_R/A_S$. This combined with Eqs. (4), (5) and (6) gives (Brabazon et al., 2019b):

$$\cos\theta_R = \left(\frac{\mathcal{L}}{\ell}\right)^{2-D_f}\cos\theta_S \tag{7}$$

Substituting Eq. (7) into Eq. (2) for the spontaneous imbibition process in a single fracture yields:

$$L_s\mathrm{d}L_s = \left[\frac{a\sigma\left(\frac{\mathcal{L}}{\ell}\right)^{2-D_f}\cos\theta_S}{6\mu\tau^2} - \frac{a^2\rho g L_s}{12\mu\tau^2}\right]\mathrm{d}t \tag{8}$$

For convenience, the following constants are defined as: $A = [a\sigma(\mathcal{L}/\ell)^{2-D_f}\cos\theta_S]/(6\mu\tau^2)$ and $B = (a^2\rho g)/(12\mu\tau^2)$. Then, the implicit analytical solution for the imbibition height can be easily obtained by integrating Eq. (8):

$$t = -\frac{A}{B^2}\ln\left(1 - \frac{B}{A}L_s\right) - \frac{L_s}{B} \tag{9}$$

Implicit analytical solutions are often inconvenient for practical applications. To address this limitation, an explicit analytical solution for imbibition height is sought here. In previous work (Fries and Dreyer, 2008; Cai et al., 2012; Wang and Cheng, 2020), an explicit solution for spontaneous imbibition height in a single fracture or capillary tube was derived by introducing the Lambert function. Similarly, in the present study, by applying the Lambert function to solve Eq. (8), an explicit analytical solution for imbibition height is obtained that incorporates surface roughness:

$$L_s(t) = \frac{A}{B}\left\{1 + W\left[-\exp\left(-1 - \frac{tB^2}{A}\right)\right]\right\} \tag{10}$$

where the Lambert function $W(x)$ can be approximated by $W(x) \approx (2\mathrm{e}x - 10.7036 + 7.56859\sqrt{2+2\mathrm{e}x})/(12.7036 + 5.13501\sqrt{2+2\mathrm{e}x})$, $-\mathrm{e}^{-1} \le x \le 0$ (e stands for Euler's number).

Although the analytical expression of the imbibition front (Eq. (10)) appears similar in form to those presented in the models of Fries and Dreyer (2008) and Wang and Cheng (2020), there are essential differences in their underlying assumptions and applicability. The model by Fries and Dreyer (2008) was derived based on the capillary tube approximation and is therefore more suitable for porous media rather than fractures. In contrast, both our model and that of Wang and Cheng (2020) are derived from the parallel-plate assumption, which is more appropriate for fracture flow. The key distinction between our model and Wang and Cheng (2020)'s lies in the consideration of fracture surface roughness. While Wang and Cheng (2020) assumed a smooth fracture surface, our model explicitly incorporates the effect of roughness through the fractal dimension D_f, which modifies the flow resistance and capillary pressure. As a result, the coefficient A in Eq. (10) differs between the two models. When $D_f = 2$, representing a smooth surface, our model reduces exactly to the form proposed by Wang and Cheng (2020), making it a special case of the generalized model presented here.

The imbibition height predictions obtained from the implicit solution (Eq. (9)) and the fully analytical solution (Eq. (10)) for the spontaneous imbibition of a single-phase fluid into a single rough fracture exhibit an almost perfect agreement, confirming the reliability and accuracy of the fully analytical formulation developed in this study (Fig. 2).

3. Model validation

The experimental data used for model validation were obtained from previously published literature (Brabazon et al., 2019b). In the experiments conducted by (Brabazon et al., 2019b), the fractures were generated by artificially splitting natural rock cores. The wetting phase (water) imbibed upward from the bottom into the initially dry fracture, inherently incorporating the effect of gravity. The fractal dimension was

Table 1. Physical parameters of fluids and fractures for modeling calculations.

Parameter	Crossville sandstone	Mancos shale
Aperture (μm)	93	87
Surface fractal dimension (-)	2.24	2.45
Tortuosity (-)	1	1.006
Contact angle of fluid on a smooth surface (°)	41.3	37.2
Fluid density (kg/m^3)	1,049.3	1,049.3
Fluid viscosity (Pa·s)	0.001	0.001
$\mathcal{L}/\ell$ (-)	100	100
Interfacial tension (N/m)	0.0728	0.0728
Gravitational acceleration (m/s^2)	9.8	9.8

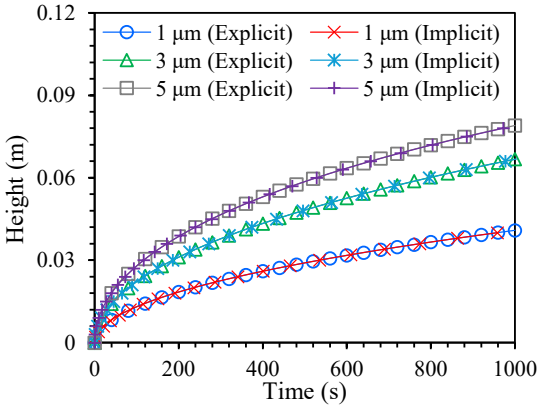

Fig. 2. Comparison of the calculation results of implicit analytical solution and explicit analytical solution (model parameter: $\sigma = 0.0728$ N/m; $\theta_S = 45°$; $\rho = 1,049.3$ kg/m^3; $\tau = 1$; $g = 9.8$ m/s^2; $D_f = 2.5$; $\mathcal{L}/\ell = 100$).

determined using the image variation method. Details of the fractal dimension measurement can be found in Brabazon et al. (2019a) and Perfect et al. (2020). The physical properties of the fluids and fractures used in the model calculations are summarized in Table 1. Specifically, the fracture aperture, surface fractal dimension, tortuosity, and the contact angle of the fluid on a smooth surface were adopted from Brabazon et al. (2019a). The fluid density and viscosity were referenced from the properties of water, while the interfacial tension was taken from air-water interfacial tension values. The value of the ratio $\mathcal{L}/\ell$ was referenced from Brabazon et al. (2019a) who used image variation methods to measure the fractal dimension of the fracture surface. The maximum and minimum grid sizes were 100,000 and 1,000 pixel units, respectively, yielding a scale ratio of 100. Thus, in this study, the ratio $\mathcal{L}/\ell$ of the side lengths between the largest and smallest squares covering the rough fracture surface was set to 100. For comparison, the imbibition height as a function of time was calculated for two cases: One with surface roughness considered and the other without. In the latter case, the surface fractal dimension D_f in the model was set to 2, implying $\cos\theta_R = \cos\theta_S$, meaning that surface roughness had no effect on the contact angle.

The model predictions and experimental results for Crossville sandstone and Mancos shale reveal that neglecting surface roughness leads to a noticeable deviation between predicted imbibition heights and measured data, whereas incorporating roughness markedly improves the agreement (Fig. 3). These findings indicate that neglecting surface roughness leads to an overestimation of the imbibition rate and a predicted final imbibition height greater than the actual value.

4. Effect of roughness on spontaneous imbibition

The above model validation results indicate that fracture surface roughness has a significant impact on imbibition behavior. This section analyzes the influence of surface roughness, characterized by the surface fractal dimension, on the fracture imbibition dynamics.

The computed imbibition height as a function of time for different surface fractal dimensions shows that, taking $D_f = 2$ (representing a smooth fracture surface) as a reference, increasing the surface fractal dimension progressively reduces both the imbibition rate and the imbibition height at any given time, which is due to the greater roughness associated with higher surface fractal dimension values (Fig. 4).

Roughness primarily influences imbibition behavior by modifying the apparent contact angle. An increase in the surface fractal dimension D_f (indicating higher roughness) amplifies the effect of the intrinsic contact angle θ_S through the Wenzel factor r, leading to a larger apparent contact angle θ_R during imbibition ($\cos\theta_R = r\cos\theta_S$). As θ_R increases, $\cos\theta_R$ decreases, reducing the capillary pressure (the primary driving force of imbibition). Consequently, a larger surface fractal dimension yields a weaker imbibition driving force, which slows the imbibition rate and reduces the imbibition equilibrium height.

The influence of contact angle on gas-water imbibition behavior in fractures was further analyzed (Fig. 5(a)). For the same contact angle, the imbibition rate in rough fractures was consistently slower than that in smooth fractures. To quantitatively characterize the difference in imbibition behavior betw-

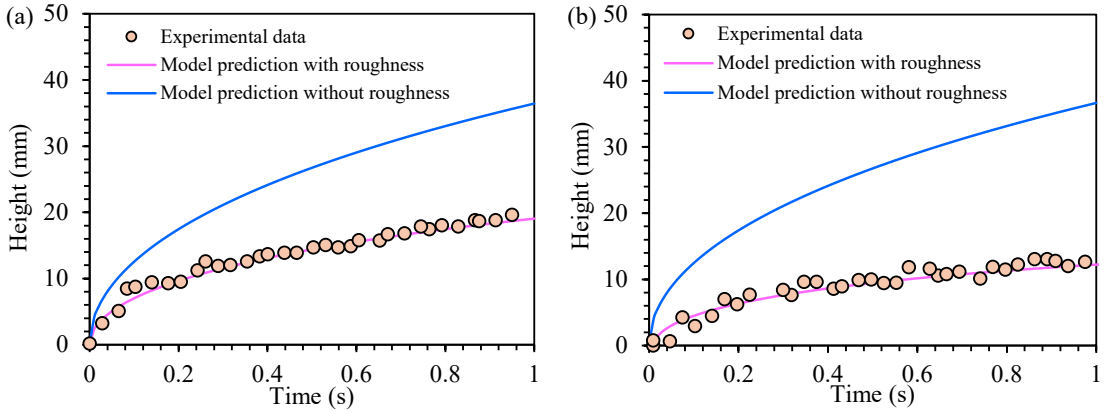

Fig. 3. Comparison of model predictions with experimental results for (a) Crossville sandstone and (b) Mancos shale.

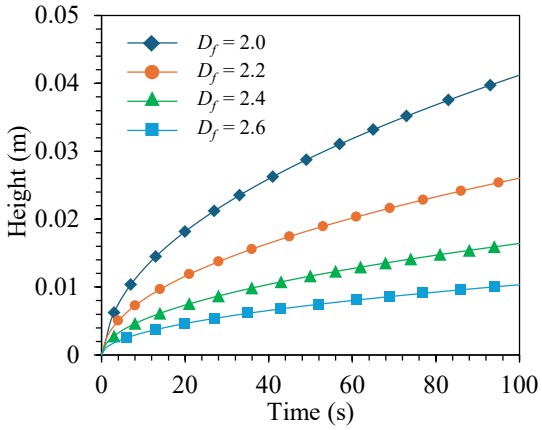

Fig. 4. Variation in imbibition height with time for different surface fractal dimensions (model parameter: $a = 1$ μm; $\tau = 1$; $\sigma = 0.0728$ N/m; $\theta_S = 45°$; $\rho = 1{,}049.3$ kg/m^3; $g = 9.8$ m/s^2; $D_f = 2.6$; $\mathcal{L}/\ell = 100$).

een rough and smooth fractures under different contact angles, the ratio of imbibition height in rough fractures to that in smooth fractures was calculated as a function of time for various contact angles (Fig. 5(b)). As the contact angle decreased from 80° to 45° and then to 10°, the height ratio-time curves shifted markedly upward, indicating that the difference in imbibition behavior between rough and smooth fractures progressively increased. This suggests that a smaller contact angle (i.e., stronger wettability of the fracture toward the wetting-phase fluid) amplifies the effect of surface roughness on gas-water imbibition behavior.

Similarly, the influence of interfacial tension on gas-water imbibition behavior was examined (Figs. 6(a) and 6(b)). Likewise, an increase in interfacial tension amplified the effect of surface roughness on imbibition behavior. As the interfacial tension increased from 0.01 to 0.1 N/m and then to 1 N/m, the height ratio-time curves shifted significantly upward, indicating a progressive increase in the difference between rough and smooth fractures. Both a decrease in contact angle and an increase in interfacial tension imply stronger wettability, which enhances capillary forces and accelerates the imbibition rate. Since surface roughness influences the imbibition process primarily by altering capillary forces, both a smaller contact angle and a higher interfacial tension indirectly strengthen the impact of surface roughness on the imbibition behavior.

Due to the presence of gravity, if the fracture height is infinitely long, the imbibition front will cease to change once it reaches a certain height (Fries and Dreyer, 2008). This final height is referred to as equilibrium height (Fries and Dreyer, 2008). When the imbibition height reaches this height, it will no longer change with time, i.e., $\mathrm{d}L_s/\mathrm{d}t = 0$. Substituting $\mathrm{d}L_s/\mathrm{d}t = 0$ into Eq. (8), the equilibrium height L_{se} can be obtained as follows:

$$L_{se} = \frac{A}{B} = \frac{2\sigma\left(\frac{\mathcal{L}}{\ell}\right)^{2-D_f}\cos\theta_S}{a\rho g} \tag{11}$$

The corresponding concept to equilibrium height is equilibrium time, which refers to the time at which the imbibition height reaches the equilibrium height. The time when $L_s = 0.99L_{se}$ can be approximated as the imbibition equilibrium time (Fries and Dreyer, 2008). Substituting $L_s = 0.99L_{se}$ into Eq. (9) yields:

$$t_e = \frac{3.62A}{B^2} = 3.62\frac{L_{se}}{B} = \frac{86.88\mu\tau^2\sigma\left(\frac{\mathcal{L}}{\ell}\right)^{2-D_f}\cos\theta_S}{a^3\rho^2 g^2} \tag{12}$$

The variations in equilibrium imbibition height and equilibrium time with respect to the surface fractal dimension, calculated using Eqs. (11) and (12), show that both parameters decrease nonlinearly as the surface fractal dimension increases (Fig. 7). This trend is mainly attributed to the capillary pressure reduction, which is the dominant driving force of imbibition and results from increased surface roughness. The use of Eqs. (11) and (12) therefore allows the quantitative evaluation of the effect of roughness on imbibition behavior, as reflected in the changes in both equilibrium height and equilibrium time.

Furthermore, the dependence of equilibrium height and equilibrium time on fracture aperture for different surface fractal dimensions was analyzed (See Fig. 8). For a given surface fractal dimension, both equilibrium height and equilibrium time decrease as fracture aperture increases. This is because a larger fracture aperture leads to a reduction in capillary pressure while simultaneously enhancing the influence of gra-

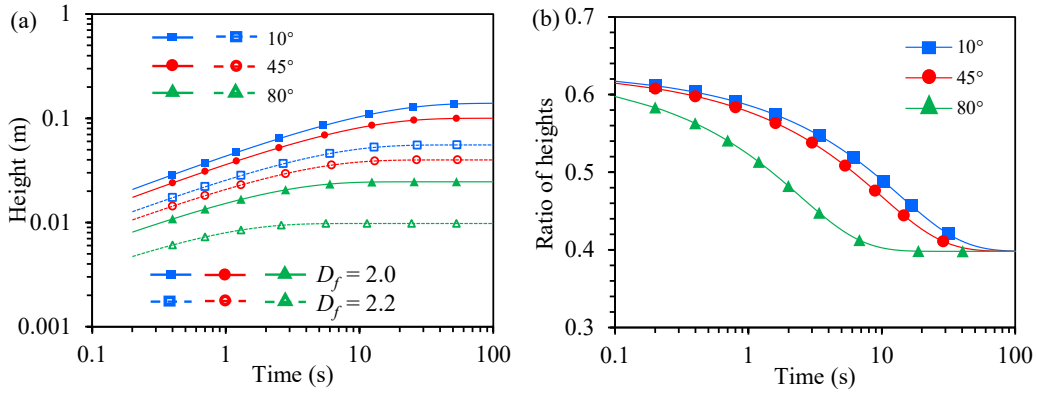

Fig. 5. (a) Effect of contact angle on the imbibition height–time curves in rough and smooth fractures and (b) variation in the ratio of imbibition height at $D_f = 2.2$ to that at $D_f = 2.0$ with time for different contact angles.

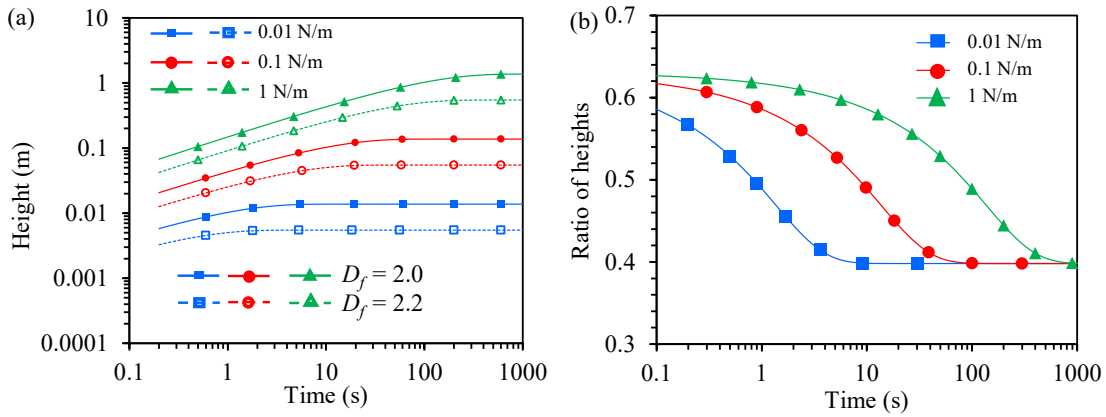

Fig. 6. (a) Effect of interfacial tension on the imbibition height–time curves in rough and smooth fractures and (b) variation in the ratio of imbibition height at $D_f = 2.2$ to that at $D_f = 2.0$ with time for different interfacial tensions.

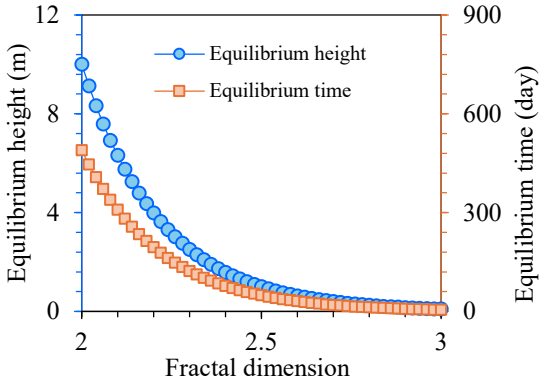

Fig. 7. Variation in equilibrium height and equilibrium time with surface fractal dimension. (Model parameters: $a = 100$ μm; $\tau = 1$; $\sigma = 0.0728$ N/m; $\theta_S = 45°$; $\rho = 1{,}049.3$ kg/m^3; $g = 9.8$ m/s^2; $\mathcal{L}/\ell = 100$).

vity on the flow. In this work, capillary pressure serves as the driving force for imbibition while gravity acts as a resistive force, therefore the observed trend is governed by the competition between these effects.

Taking $D_f = 2$ (representing smooth fracture surface) as a reference, it is evident that as the surface fractal dimension increases (representing increased roughness), the equilibrium height and equilibrium time decrease for the same fracture aperture. Moreover, the rate at which equilibrium height and equilibrium time decline with increasing fracture aperture becomes more pronounced as roughness increases. This observation highlights that fracture surface roughness essentially acts as a resistance to imbibition flow, further exacerbating the reduction in equilibrium height and equilibrium time with increasing fracture aperture.

5. Conclusions

This study investigated spontaneous air-water imbibition in rough fractures by establishing a mathematical model that incorporates the effects of both fracture surface roughness and gravity. The influence of surface roughness on imbibition behavior was systematically analyzed, leading to the following conclusions:

1) Lambert function is an effective tool for obtaining a fully analytical solution for imbibition height in air-water spontaneous imbibition while accounting for gravity. The imbibition height calculated using the fully analytical solution derived from the Lambert function exhibits no significant deviation from the implicit analytical solution.
2) A comparison between experimental data and model predictions demonstrates that fracture surface roughness has a significant impact on imbibition behavior. Neglecting

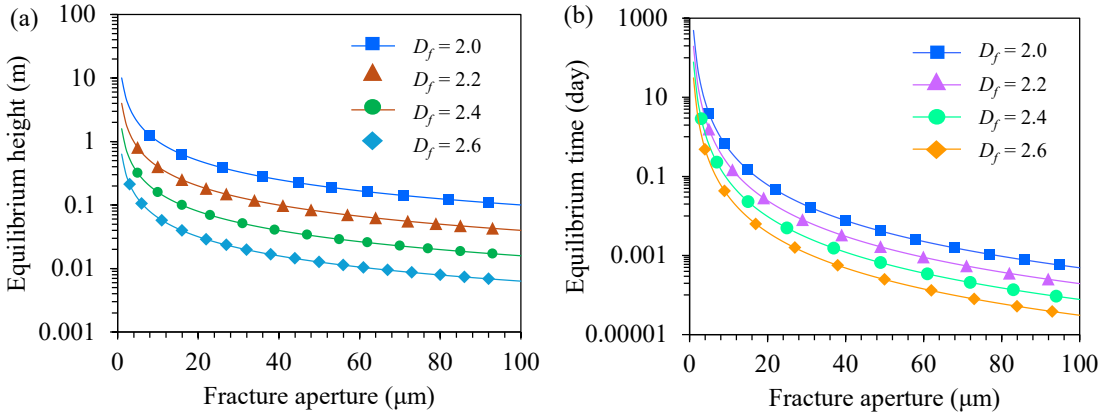

Fig. 8. (a) Variation in equilibrium height and (b) equilibrium time with fracture aperture for different surface fractal dimensions. For the definitions of L_{se} and t_e, as well as the model parameter values, see Fig. 7.

roughness leads to an overestimation of the imbibition rate and a predicted equilibrium imbibition height that is greater than the actual value.

3) As the surface fractal dimension increases, the imbibition rate decreases and the imbibition height at any given time is also reduced. A decrease in contact angle and an increase in interfacial tension both amplify the effect of surface roughness on gas-water imbibition behavior in fractures. Both equilibrium height and equilibrium time decrease with increasing surface fractal dimension.

It should be noted that the present model focuses solely on spontaneous air-water imbibition within rough fractures and neglects fluid exchange between the fracture and the surrounding matrix. While this simplification enables a clearer analysis of the effects of roughness and gravity on the imbibition process, it also limits the applicability of the model to real geological systems where matrix-fracture interactions may play a significant role. Thus, future work should aim to incorporate matrix-fracture fluid exchange to better capture the complexity of natural systems.

Acknowledgements

This research was supported by the China National Science Foundation (Nos. 42472320 and U2244215).

Conflict of interest

The authors declare no competing interest.

References

Abd, A. S., Elhafyan, E., Siddiqui, A. R., et al. A review of the phenomenon of counter-current spontaneous imbibition: Analysis and data interpretation. Journal of Petroleum Science and Engineering, 2019, 180: 456-470.

Andersen, P. O. Early- and late-time prediction of counter-current spontaneous imbibition, scaling analysis and estimation of the capillary diffusion coefficient. Transport in Porous Media, 2023, 147(3): 573-604.

Brabazon, J. W., Perfect, E., Gates, C. H., et al. Rock fracture sorptivity as related to aperture width and surface roughness. Vadose Zone Journal, 2019a, 18: 180156.

Brabazon, J. W., Perfect, E., Gates, C. H., et al. Spontaneous imbibition of a wetting fluid into a fracture with opposing fractal surfaces: Theory and experimental validation. Fractals-Complex Geometry Patterns and Scaling in Nature and Society, 2019b, 27(1): 1940001.

Cai, J., Chen, Y., Liu, Y., et al. Capillary imbibition and flow of wetting liquid in irregular capillaries: A 100-year review. Advances in Colloid and Interface Science, 2022, 304: 102654.

Cai, J., Hu, X., Standnes, D., et al. An analytical model for spontaneous imbibition in fractal porous media including gravity. Colloids and Surfaces a-Physicochemical and Engineering Aspects, 2012, 414: 228-233.

Cai, J., Qin, X., Wang, H., et al. Pore-scale investigation of forced imbibition in porous rocks through interface curvature and pore topology analysis. Journal of Rock Mechanics and Geotechnical Engineering, 2025, 17(1): 245-257.

Cheng, H., Wang, F. Effects of gravity and buoyancy on spontaneous liquid-liquid imbibition in fractured porous media. Capillarity, 2024, 10(1): 1-11.

Family, F., Vicsek, T. Dynamics of fractal surfaces. Fractal Concepts in Surface Growth, 1991.

Fries, N., Dreyer, M. An analytic solution of capillary rise restrained by gravity. Journal of Colloid and Interface Science, 2008, 320(1): 259-263.

Guo, J., Zhao, Y., He, L., et al. Spontaneous imbibition of unsaturated sandstone under different vertical temperature gradients: Neutron radiography experiments and dynamic models. Advances in Water Resources, 2024, 193: 104832.

Hu, Y., Xu, W., Zou, L., et al. Evaluating the long-term barrier performance of fractured granite for nuclear waste disposal: Impact of fast water-conducting path. Engineering Geology, 2024, 337: 107583.

Janetti, M. B., Janssen, H. Effect of dynamic contact angle

variation on spontaneous imbibition in porous materials. Transport in Porous Media, 2022, 142(3): 493-508.

Khan, J., Padmanabhan, E., Ul Haq, I., et al. Hydraulic fracturing with low and high viscous injection mediums to investigate net fracture pressure and fracture network in shale of different brittleness index. Geomechanics for Energy and the Environment, 2023, 33: 100416.

Ma, G., Ma, C., Chen, Y., et al. An equivalent model for fluid flow along a rough-walled fracture considering the effect of the multi-scale roughness and internal contacts. Geoenergy Science and Engineering, 2025, 247: 213677.

Meng, Q., Liu, H., Wang, J., et al. Effect of gravity on spontaneous imbibition from cores with two ends open in the frontal flow period. Journal of Petroleum Science and Engineering, 2016, 141: 16-23.

Minakov, A., Pryazhnikov, M., Neverov, A., et al. Wettability, interfacial tension, and capillary imbibition of nanomaterial-modified cross-linked gels for hydraulic fracturing. Capillarity, 2024, 12(2): 27-40.

Munoz, L., Mejia, C., Rueda, J., et al. Iterative coupling of DDM and FEM for planar hydraulic fracturing under non-uniform confining stresses. Computers and Geotechnics, 2025, 186: 107432.

Nazridoust, K., Ahmadi, G., Smith, D. A new friction factor correlation for laminar, single-phase flows through rock fractures. Journal of Hydrology, 2006, 329(1-2): 315-328.

Perfect, E., Brabazon, J. W., Gates, C. H. Forward prediction of early-time spontaneous imbibition of water in unsaturated rock fractures. Vadose Zone Journal, 2020, 19(1): e20056.

Rezaei, A., Mousavi, Z. Characterization of land deformation, hydraulic head, and aquifer properties of the gorgan confined aquifer, iran, from insar observations. Journal of Hydrology, 2019, 579: 124196.

Salam, A., Wang, X. An analytical solution on spontaneous imbibition coupled with fractal roughness, slippage and gravity effects in low permeability reservoir. Journal of Petroleum Science and Engineering, 2022, 208: 109501.

Shi, Y., Yassin, M., Dehghanpour, H. A modified model for spontaneous imbibition of wetting phase into fractal porous media. Colloids and Surfaces a-Physicochemical and Engineering Aspects, 2018, 543: 64-75.

Srivastava, M. K., Kishor, K., Singh, A. K., et al. Tectonically deformed coal: Focus on microstructures & implications for basin evolution. Marine and Petroleum Geology, 2025, 172: 107223.

Standnes, D. C. Analysis of oil recovery rates for spontaneous imbibition of aqueous surfactant solutions into preferential oil-wet carbonates by estimation of capillary diffusivity coefficients. Colloids and Surfaces A: Physicochemical and Engineering Aspects, 2004, 251(1-3): 93-101.

Torkan, M., Uotinen, L., Baghbanan, A., et al. Experimental and numerical characterization of hydro-mechanical properties of rock fractures: The effect of the sample size on roughness and hydraulic aperture. International Journal of Rock Mechanics and Mining Sciences, 2025, 186: 106009.

Wang, F., Cheng, H. Effect of gravity on spontaneous imbibition of the wetting phase into gas-saturated tortuous fractured porous media: Analytical solution and diagnostic plot. Advances in Water Resources, 2020, 142: 103657.

Wang, F., Cheng, H., Song, K. A mathematical model of surfactant spontaneous imbibition in a tight oil matrix with diffusion and adsorption. Langmuir, 2021, 37(29): 8789-8800.

Washburn, E. W. The dynamics of capillary flow. Physical Review Journal, 1921, 17(3): 273-283.

Wenzel, R. N. Resistance of solid surfaces to wetting by water. Transactions of the Faraday Society, 1936, 28(8): 988-994.

Wolansky, G., Marmur, A. Apparent contact angles on rough surfaces: The wenzel equation revisited. Colloids and Surfaces A: Physicochemical and Engineering Aspects, 1999, 156(1-3): 381-388.

Wu, M., Jiang, C., Song, R., et al. Comparative study on hydraulic fracturing using different discrete fracture network modeling: Insight from homogeneous to heterogeneity reservoirs. Engineering Fracture Mechanics, 2023, 284: 109274.

Xia, Y., Tian, Z., Xu, S., et al. Effects of microstructural and petrophysical properties on spontaneous imbibition in tight sandstone reservoirs. Journal of Natural Gas Science and Engineering, 2021, 96: 104225.

Yaghoubi, A. Hydraulic fracturing modeling using a discrete fracture network in the barnett shale. International Journal of Rock Mechanics and Mining Sciences, 2019, 119: 98-108.

Yoon, W. W., Han, W. S., Hwang, J., et al. Effect of fracture characteristics on groundwater flow adjacent to high-level radioactive waste repository. Journal of Hydrology, 2024, 629: 130593.

Zhang, J., Chen, J., Zhao, Z., et al. Numerical modeling on nuclide transport around a nuclear waste repository under coupled thermo-hydro-mechanical condition. Computers and Geotechnics, 2023a, 164: 105776.

Zhang, S., Liu, X. A semi-analytical solution for the equivalent permeability coefficient of the multilayered porous medium with continuous fracture. Water Resources Research, 2024, 60(2): e2023WR036203.

Zhang, S., Liu, X., Wang, E. Quantitative evaluation of the onset and evolution for the non-darcy behavior of the partially filled rough fracture. Water Resources Research, 2024a, 60(3): e2023WR036494.

Zhang, S., Liu, X., Wang, E., et al. A novel model of hydraulic aperture for rough single fracture: Insights from fluid inertial and fracture geometry effects. Journal of Geophysical Research-Solid Earth, 2024b, 129(7): e2024JB029018.

Zhang, X., Ye, Q., Deng, J., et al. Experimental study and mechanism analysis of spontaneous imbibition of surfactants in tight oil sandstone. Capillarity, 2023b, 7(1): 1-12.

Zhou, W., Kulenkampff, J., Heredia, D. J., et al. Variability of fracture surface roughness in crystalline host rocks: Implications for transport model simplifications. Applied Geochemistry, 2025, 186: 106401.